ORIGINAL ARTICLE

Environmental protection and performance enhancement of hydrocarbon compressor based vapour compression refrigeration system using dry powder SiO$_2$ nanoparticles: an experimental analysis

Navdeep Kumar[1,3] · Pardeep Kumar[2] · Khushdeep Goyal[3]

Abstract

The present research explores the dispersion of SiO$_2$ nanoparticles in compressor lubricant, polyolester (POE) oil for performance enhancement of vapour compression refrigeration system (VCRS). The contribution of SiO$_2$ nanoparticles based nanolubricant was examined for eco-friendly hydrocarbon (HC) refrigerant R600a, retrofitted to hydrofluorocarbon (HFC) compressor based VCRS and also in HC compressor, in governing the performance of VCRS. Wear characteristics improved by the nanolubricants were assessed through pin-on-disc wear testing, using the pins extracted from the actual compressor piston used in VCRS. As compared to POE oil, the average specific wear rate (SWR) and coefficient of friction (COF) of nanolubricant were reduced by about 20% and 29%, respectively. Enhanced average viscosity and average thermal conductivity were observed (35–95 °C), with maximum increases of about 13% at 65 °C and 45% at 95 °C, respectively, in comparison to those of POE oil. Field emission scanning electron microscopy (FE-SEM) was utilized to analyze the morphology of SiO$_2$ nanoparticles, while Fourier transform infrared spectroscopy (FTIR) and X-ray diffraction (XRD) analyzed their crystal structure. The Zeta potential tests for the prepared nanolubricant were conducted to ensure its long-term stability. An HC compressor based VCRS shows better performance including average refrigeration effect, average power consumption by compressor, and the average coefficient of performance (COP) of 29%, 7%, and 39%, respectively compared to the base lubricant filled retrofitted system. Hence the findings of the present research provide novel perspectives on the potential benefits of incorporating SiO$_2$ nanoparticles and an HC compressor to improve the VCRS performance.

Keywords VCRS · Nanolubricant · HC R600a · SiO$_2$ nanoparticles · POE oil

Abbreviations

COF	Coefficient of friction
COP	Coefficient of performance
EDS	Energy dispersive spectroscopy
FE-SEM	Field emission scanning electron microscope
FF	Friction force
FTIR	Fourier transform infrared
GWP	Global warming potential
HC	Hydrocarbon
HFC	Hydrofluorocarbon
nm	Nanometer
ODP	Ozone depletion potential
POE	Polyolester
rpm	Revolutions per minute
SiO$_2$	Silicon dioxide
SWR	Specific wear rate
VCRS	Vapour compression refrigeration system
XRD	X-ray diffraction

Symbols [unit]

C_p	Specific heat capacity of water [kJkg^{-1} K^{-1}]
K	Energy meter constant [Impulse kW^{-1} h^{-1}]
n	Number of pulses taken by the energy meter
m	Mass of water [kg]
t	Time period over which the pulses are counted [sec.]
ΔT	Temperature difference [K]
ϕ	Diameter
°C	Degree Celsius

✉ Navdeep Kumar
   nav9303@yahoo.com

1   Department of Mechanical Engineering, Guru Kashi University, Talwandi Sabo, Bathinda, Punjab 151302, India

2   Yadavindra Department of Engineering, Punjabi University Guru Kashi Campus, Talwandi Sabo, Bathinda, Punjab 151302, India

3   Department of Mechanical Engineering, Punjabi University, Patiala, Punjab 147002, India

Springer

gL^{-1}	Grams per litre
Lh^{-1}	Litre per hour
kPa	Kilopascal
W	Watt

Subscripts

1	Compressor inlet
2	Compressor outlet

Introduction

The vapour compression refrigeration system (VCRS), commonly used in domestic and commercial refrigerators worldwide, consumes around 15% of global energy demand (Nair et al. 2020; Yıldız et al. 2021). The researchers continually tried to develop energy-efficient techniques without changing the existing components of the VCRS (Gupta et al. 2020). The environmental aspect has equal weightage to the energy concern. The VCRS employed conventional, environmentally harmful refrigerants having global warming potential (GWP) and ozone depletion potential (ODP) on the higher side, resulting in global warming and damage to the ozone layer, respectively (D.S Adelekan et al. 2019a). To address these concerns, eco-friendly refrigerants and nano-sized solid particles are adopted (Jatinder et al. 2019; Babarinde et al. 2020). Hydrocarbons (HCs) are considered one of the eco-friendly refrigerants that have low GWP and ODP index (Adelekan et al. 2019a; b). These are considered alternatives to the conventional refrigerants for the VCRS (Fatouh and Abou-Ziyan 2018; Jatinder et al. 2019; Ohunakin et al. 2018), despite their flammability concern (Adelekan et al. 2021; Ohunakin et al. 2018; Harby 2017). In addition, the higher latent heat of HCs offers the advantage of less amount charged compared to halogenated refrigerants (Rasti et al. 2013). The refrigerant R600a was used as one of the effective eco-friendly HC refrigerants, compatible with HFC compressor based VCRS (Babarinde et al. 2019; Cao et al. 2021; Akhavan-Behabadi et al. 2015). The literature shows that HC R600a is more efficient than other HC refrigerants (Jatinder et al. 2019; Ghorbani et al. 2017). In addition, the selection of compressor lubricant has a significant impact on the performance parameters, such as refrigeration effect, power consumption by compressor, and coefficient of performance (COP) of the VCRS (Soliman et al. 2018; Akhavan-Behabadi et al. 2015). The polyolester (POE) oil, one of the compressor lubricants, has good miscibility and is compatible with HC R600a refrigerant (Akhavan-Behabadi et al. 2015), good thermal and chemical stability with system components, and maintains its lubricating properties across a broader temperature range (Chauhan et al. 2019). The experiment results of Soliman et al. (2018) reveal that POE oil-based nanolubricant performed better than mineral oil-based nanolubricant.

The thermal conductivity of fluids can be enhanced by dispersing solid nanoparticles having relatively high thermal conductivity, which further increases their heat transfer capacity (Ibrahim Khan et al. 2019a; Yıldız et al. 2021; Gupta et al. 2015). The concept of dispersing solid particles (milli-meter and micro-meter) in the heat transfer fluid was investigated about a century ago, to improve upon the thermophysical properties of the fluids (Narayanasarma and Kuzhiveli 2019; Kotia et al. 2017; Okonkwo et al. 2020). However, this kind of fluid poses a major issue of stability which leads to the clogging of the system (Gupta et al. 2015). To overcome the challenges, Steve Choi in 1995 dispersed the nanoparticles (size under 100 nm) into the base fluid and termed it a "nanofluid" (Sanukrishna et al. 2019; Sanukrishna and Prakash 2018; Mansourian et al. 2020). A nanofluid, prepared by dispersing various types of nanoparticles in a base fluid, is considered a novel fluid (Devendiran and Amirtham 2016; Ibrahim Khan et al. 2019a). The nanosize of the particles dispersed in the base fluid offers unobstructed flow through all passages of the thermal systems (Sharif et al. 2016; Okonkwo et al. 2020). Literature also witnesses the higher thermal conductivity of the prepared nanofluids than their respective base fluids (Zawawi et al. 2017; Xiaohao Wei et al. 2009). Moreover, the shape and crystal structure of the dispersed nanoparticles significantly impacts the thermophysical and tribological properties of the prepared nanolubricant (Alawi et al. 2018; Xiaohao Wei et al. 2009).

In VCRS, appending distinct nanoparticles through compressor lubricant (known as 'nanolubricant') or refrigerant (known as 'nanorefrigerant') (Sharif et al. 2018; Nair et al. 2020), are the viable methods of energy-saving and performance enhancement. Mostly, nanolubricant is preferred, as it is more challenging to mix nanoparticles into the refrigerant (Nair et al. 2020). The next challenge in this direction is the stability of the prepared nanolubricant. Nanolubricant stability is vital for maximizing its benefits as an effective heat transfer fluid across various thermal systems (Abdel-Hadi et al. 2016). It is considered a key parameter before considering an effective compressor lubricant for VCRS (Ravinder Kumar et al. 2022). In general, cohesive, Van der Waals forces increase the tendency of particles to agglomerate (Sidik et al. 2014; Hatami and Jing 2020; Okonkwo et al. 2020). This further leads to the instability of the prepared nanolubricant (Mansourian et al. 2020). To address this challenge, magnetic stirring, and bath ultrasonication were employed for specific durations (Yilmaz 2020; Sanukrishna et al. 2018; Narayanasarma and Kuzhiveli 2019). Zeta potential analysis of prepared nanolubricants

is a commonly preferred method for stability analysis, often adopted by researchers (Le Ba et al. 2020; Chakraborty and Panigrahi 2020).

The literature also shows the benefits of the use of TiO$_2$ nanoparticles to prepare nanolubricant for VCRS performance enhancement (Adelekan et al. 2019b; Sabareesh et al. 2012; Padmanabhan and Palanisamy 2012; Jatinder et al. 2019; Babarinde et al. 2019). However, its prolonged use may pose a safety concern in a VCRS, due to its high dielectric constant (≈ 80) (Nair et al. 2020). On the other hand, SiO$_2$ nanoparticles having a low value of dielectric constant (≈ 20) (Robertson 2004; Sia et al. 2014) may be used much more safely in VCRS. The low dielectric constant of SiO$_2$ nanoparticles offers one of the advantages of protecting the hermetic-type compressor against premature failure caused by electric shocks (Sia et al. 2014). Furthermore, the SiO$_2$ nanoparticles are non-toxic, chemically stable, safe, and non-reactive with the compressor lubricant and the system components (Narayanasarma and Kuzhiveli 2019). Moreover, the anti-friction, resistance to wear, and the ability to bear high load capacity of SiO$_2$ nanoparticles make the compressor base lubricant more capable of enhancing the performance of VCRS (Goto and Honda 2004; Sia et al. 2014; Patil et al. 2013a). In addition, their good tribological properties in contrast to other frequently employed nanoparticles such as TiO$_2$, Al$_2$O$_3$, ZnO, CuO, and ZrO$_2$ (Rawat et al. 2018), make them a promising candidate for preparing the nanolubricant to enhance the performance of the VCRS. The literature witnesses the enhancement of VCRS performance by dispersing the SiO$_2$ nanoparticles into the compressor lubricant which improves its tribological and thermophysical properties (Kotia et al. 2019; Patil et al. 2013b; Sanukrishna et al. 2019; Narayanasarma and Kuzhiveli 2019).

To critically analyze the contribution of the nanoparticles, in a nanolubricant, in reducing the power consumption in a VCRS, the friction characteristics need to be studied (Kotia et al. 2019; Singh et al. 2020). The coefficient of friction (COF) directly governs frictional work loss, which becomes a major factor for work loss if left unaddressed. There is a dire need to carry-out wear testing and analysis to obtain friction characteristics of the actual compressor material (if possible) with the prepared nanolubricants. Such kind of work is hard to find in the literature for the applications of VCRS. In addition to the selection of appropriate nanoparticles for the preparation of nanolubricants, the selection of compressor also has an equal weightage in addressing the energy-saving and environmental issues of VCRS. Compressors originally designed for HFC-based refrigerants are often retrofitted with HC refrigerants to improve the performance of VCRS (Bi et al. 2011; Sabareesh et al. 2012; Jatinder et al. 2019). However, for prolonged use, the performance of VCRS using an HC compressor needs to be explored while using the nanolubricants to assess whether the ease of retrofitting is justified as compared to the use of an HC compressor. A limited literature is available on the utilization of an HC compressor instead of an HFC compressor in VCRS.

As compared to TiO$_2$, SiO$_2$ nanoparticles seem to be a better alternative from a safety point of view. Further, its properties suitable for its dispersion in POE oil trigger an idea of carrying out research (limited available in the literature) with SiO$_2$ nanoparticles based nanolubricant in VCRS. For a precise analysis of the effect of SiO$_2$ nanoparticles in governing the performance parameters of the VCRS, a wear test using the actual material needs to be conducted. In addition, retrofitting looks to be an attractive option using the eco-friendly refrigerant R600a in existing VCRS. Therefore, there is a dire need to compare the VCRS system with the HC compressor to a retrofitted system, both utilizing the same HC refrigerant (R600a) and SiO$_2$ nanoparticles based nanolubricant. Therefore, the wear analysis of the actual compressor piston material using POE oil and the prepared nanolubricant, along with the use of an HC compressor instead of an HFC compressor in the VCRS test rig, highlights the gap in this research area and the novelty of the current work. Moreover, the analysis of the shape and crystal structure of nanoparticles, tribological and thermophysical properties of each lubricant sample, and stability analysis of the prepared nanolubricant sample need to be explored and correlated with the performance parameters of the VCRS.

In the present research, the morphology and crystal structure of SiO$_2$ nanoparticles were confirmed using field emission scanning electron microscope (FE-SEM), X-ray diffraction (XRD), and Fourier transform infrared (FTIR) spectroscopy. The experiments were performed with POE oil and prepared nanolubricant on an HFC compressor based retrofitted and HC compressor based VCRS test rig to examine their performance parameters. The Zeta potential test was performed to ensure nanolubricant stability. Wear tests using the actual compressor piston material were preferred to find the COF and specific wear rate (SWR). The viscosity and thermal conductivity of each lubricant sample were measured over a temperature range of 35–95 °C.

Experimental procedures

Materials

The dry SiO$_2$ nanoparticles (make: Reinste Nano Ventures Private Limited) having size 55 ± 5 nm, molecular weight 60.08 g.mol^{-1}, and density 2.6 g.cm^{-3} with 99.99% purity were used to prepare the nanolubricant. The morphologies of SiO$_2$ nanoparticles were analyzed by utilizing FE-SEM (Carl Zeiss, Merlin), while crystal structure was analyzed using FTIR spectroscopy (Tensor 27, Bruker) and XRD

diffractometer (PANalytical, Empyrean, Netherlands). The HC refrigerant R600a and the compressor lubricant POE oil were obtained from the nearby local supplier.

Nanolubricant preparation

The preparation of stable nanolubricant is not mere a mixing of a solid and liquid (Baojie. Wei et al. 2017). In this research, nanolubricant was formulated by adopting a two-step method (Yang et al. 2020; Kaggwa and Carson 2019; Borode et al. 2019). For preparation of nanolubricant small quantity of dry SiO_2 nanoparticles (0.1 gL^{-1}) were dispersed into 250 mL of compressor lubricant (POE oil). A digital readout weighing scale (CX 220, Citizen) having 0.001 g of precision was used to weigh the SiO_2 nanoparticles. The magnetic stirrer (Fig. 1) and bath ultrasonicator (Fig. 2) were utilized for 2 and 3 h, respectively (Ravinder Kumar and Singh 2016) to make nanolubricant stable and fit for its use as a compressor lubricant for a long tenure. No surfactant was used to stabilize the nanolubricant due to its potential adverse effects on VCRS performance and properties of the refrigerant used (Ravinder Kumar et al. 2020; Sanukrishna et al. 2019; Akhavan-Behabadi et al. 2015). The POE oil (base lubricant) is assigned as sample K1, while the prepared nanolubricant is designated as sample K2.
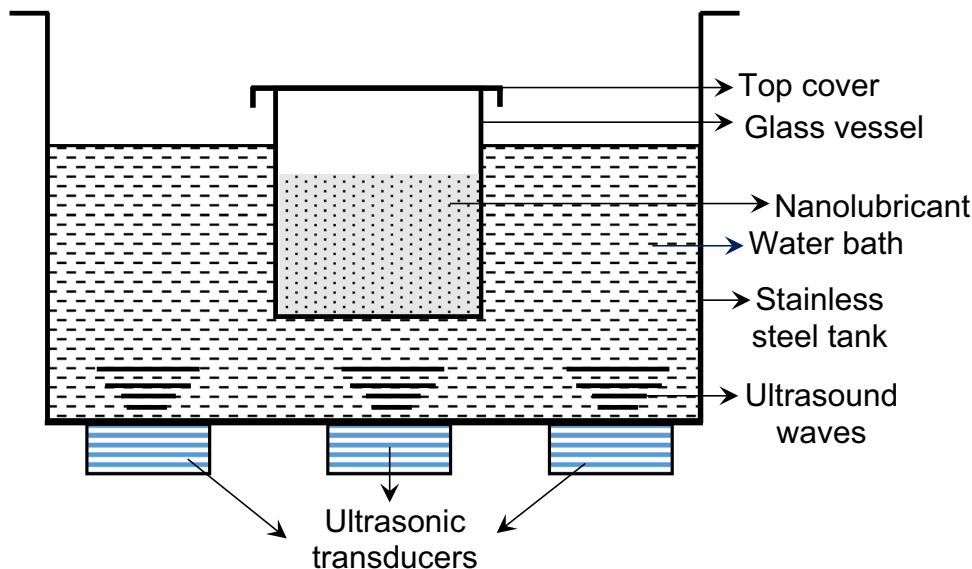
Nanolubricant stability measurement

The Zeta potential analysis was carried out to analyze the stability of the prepared nanolubricant. A Zetasizer Nano (ZS90, Malvern) was employed for a duration of 10 days, with measurements taken at a 2-day interval.

Fig. 1 Schematic diagram of magnetic stirring of nanolubricant
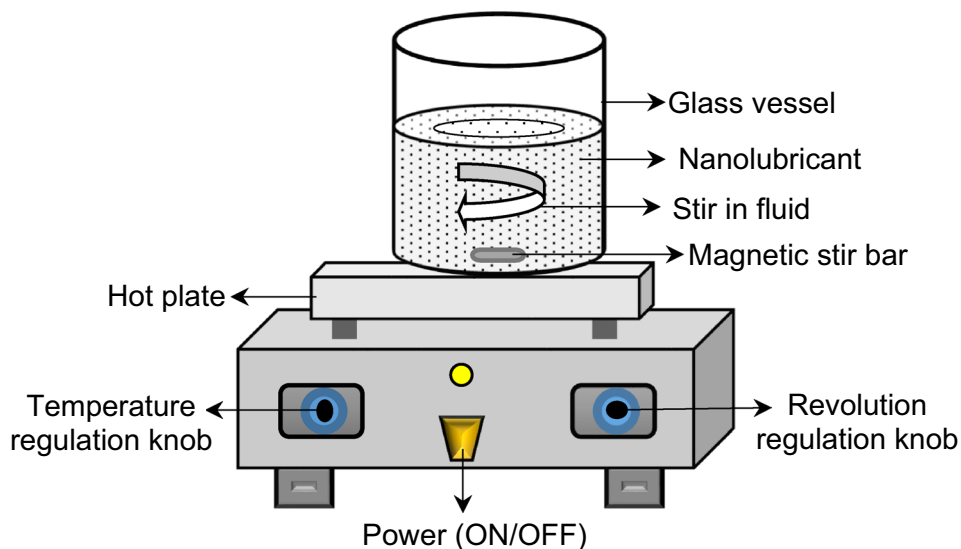
Fig. 2 Schematic diagram of bath ultrasonication of nanolubricant

Thermal conductivity measurement

The KD2 pro thermal analyzer (make: Decagon Devices, USA) was used to measure the thermal conductivity of both compressor lubricant samples, K1 and K2, as schematically shown in Fig. 3. The device was working on the principle of the 'transient hot-wire method' and also follows the ASTM D5334 standard (Narayanasarma and Kuzhiveli 2019; S.S. Sanukrishna and Prakash 2018; Hamid et al. 2018; Asadi et al. 2019). During the test, a calibrated single-needle probe (KS-1, 1.3 mm diameter, 60 mm length) was inserted into the top of the sample glass tube. Equilibrium at a constant temperature was achieved in about 15 min. Prior to each test, the probe underwent calibration using standard glycerine (CAS 56-81-5) (Zawawi et al. 2017; Sanukrishna and Prakash 2018; Narayanasarma and Kuzhiveli 2019). A water bath with constant water temperature (measured using a thermometer) was utilized to perform the test in the temperature range of 35–95 ℃. After reaching equilibrium temperature, five measurements were averaged per sample, to establish precise measurements.

Viscosity measurement test

The viscosity was measured with the help of a Redwood viscometer. The schematic diagram is shown in Fig. 4. This device operates on the principle of gravitational flow through a capillary tube with standard dimensions under

Fig. 3 Schematic of experiment setup for measurement of thermal conductivity of each sample using KD2 pro thermal analyzer
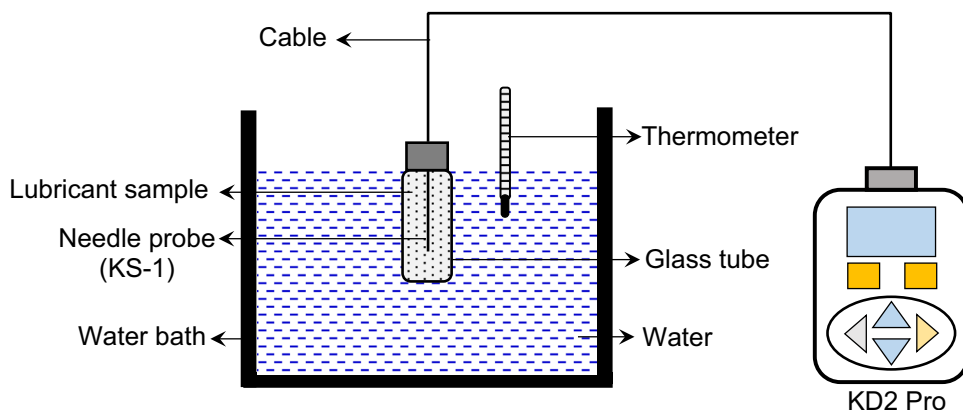
Fig. 4 Schematic of viscosity measurement with Redwood viscometer
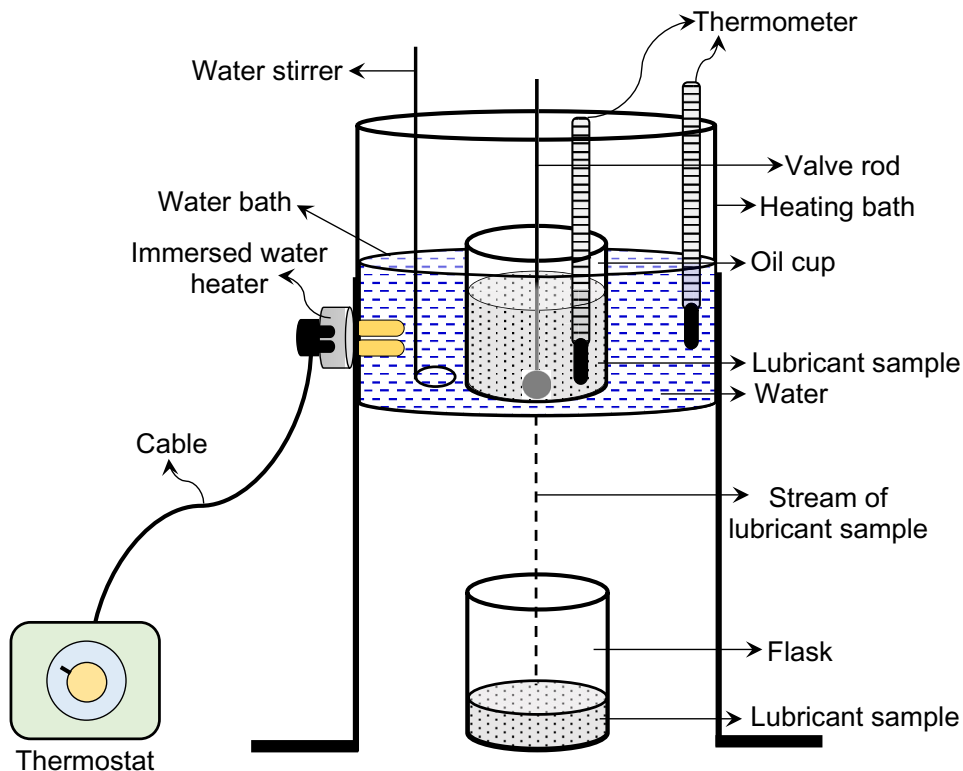
Table 1 Specifications of pin-on-disc tribometer

Parameter	Range
Applied load (normal)	0–200 N, by dead weights
FF measurement	0–200 N, least count 0.1 N
Wear measurement	0–2000 μm, least count 1 μm
Disc rotational speed	200–2000 rpm, in step of 1 rpm
Wear disc size	ϕ165 mm $\times$ 8 mm thick
Wear track diameter	Max. 140 mm, in step of 2 mm
Specimen (pin) size	ϕ3 to 12 mm, up to 32 mm long
Operating humidity	30–80%

the influence of a descending load (Sabareesh et al. 2012; Ravinder Kumar et al. 2020; Ravinder Kumar and Singh 2016). For temperature consistency across each test sample, a water bath with a submerged electric heater was used. An electric heater, controlled by a thermostat, facilitated precise temperature control throughout the experiment. To ensure uniformity, a stirrer was used in the water bath. Separate thermometers were used to measure the temperatures of both the water bath and the samples (K1 or K2) during each viscosity test. This meticulous temperature monitoring ensured that the testing took place under the desired constant temperatures of 35, 50, 65, 80, and 95 °C. Each reported viscosity value is the result of averaging the five separate measurements at each test temperature for both lubricant samples.
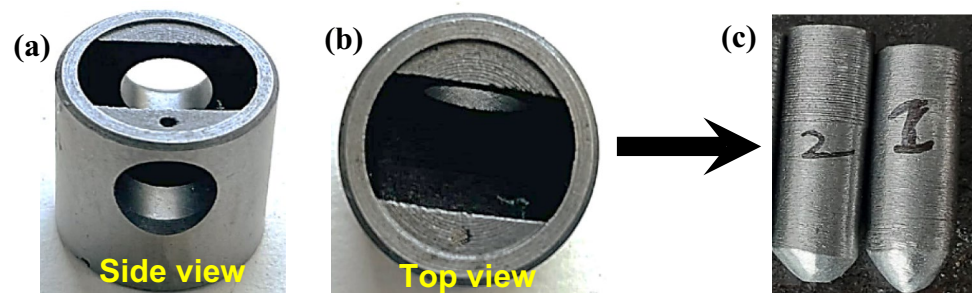
Pin-on-disc tribometer tester

The pin-on-disc tribometer (TR-20LE-PHM-CHM-550, DUCOM India) works as per ASTM-G-99 standard (Laad and Jatti 2018; Kong et al. 2022; Sabareesh et al. 2012), was employed to determine the COF and SWR. The specifications of the tribometer, used for pin-on-disc wear testing are given in Table 1. To simulate the actual conditions in

the compressor, for pin-on-disc wear testing, the pin specimens were extracted from the actual piston material of the compressor used in the VCRS test rig. The schematic of extracting the wear testing pins from the actual piston is shown in Fig. 5 and one end of each pin was machined to give it a hemispherical shape. The chemical composition of the pin material, obtained through FE-SEM/EDS analysis, is shown in Table 2.

During pin-on-disc wear testing, the pin was held firmly in the pin-holder in a vertical position to establish contact of the hemispherical end of the pin with the rotating disc at a radial distance of 70 mm. The wear testing was performed at ambient temperature and during each test, the mating surfaces were lubricated with each kind of lubricant sample with the help of an oil dispenser as shown in Fig. 6. Using dead weights, a fixed load of 98 N (F_N) was applied through the pin on the horizontal rotating disc (material: EN31 hardened to 60HRc). The testing was done for a sliding distance of 1005 m at a fixed rotating speed of 400 rpm. During the respective wear tests for each kind of lubricant samples K1 and K2, a fixed flow of 0.15 Lh^{-1} was maintained at the pin-disc interface using an oil dispenser. Due care was taken during each test to ensure the continuous supply of respective lubricant samples (K1 and K2) to the mating surfaces to avoid dry sliding. No external pressure was applied to the oil dispenser, and the lubricant film on the mating surfaces formed naturally due to the gravity-assisted flow of the lubricant. A similar procedure was adopted by Yilmaz (2020), Ingole et al. (2013), and Sabareesh et al. (2012) during wear testing of some other materials.

During each experiment of 8 min, the values of friction force (FF) were recorded at successive intervals of one minute each. The FF was measured automatically using a computer-controlled pin-on-disc tribometer and was displayed on a digital meter. The average COF was calculated from the FF data for each test. To determine SWR, the specimen's (pin) weight loss was calculated from the weight measurement
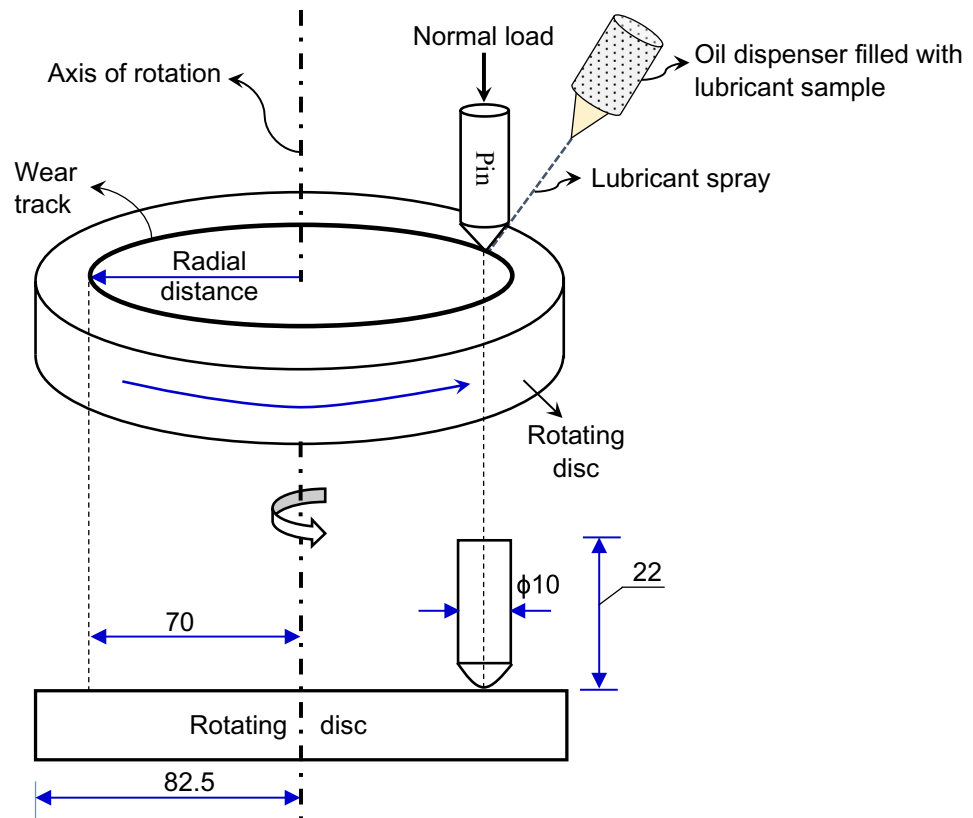
Fig. 5 **a** Side view of the compressor piston. **b** top view of the compressor piston. **c** actual pins extracted from compressor piston

Table 2 Chemical composition of pin material (weight %) as obtained through FE-SEM/EDS

C	O	Al	S	Ca	P	Fe
22.75	8.45	0.47	1.51	0.66	1.48	64.68

Springer

Fig. 6 Schematic diagram of pin–on–disc tribometer (all dimensions in mm)

data before and after each 8-min test. For precise measurements, an accurate digital weighing device having the least count of 0.001 g was used. The SWR was calculated using Eq. 1 (Kumar et al. 2021). After each test, the surface of the disc was cleaned with the help of emery paper and acetone. Each test was repeated five times under identical conditions and the reported results are the average of the five values.
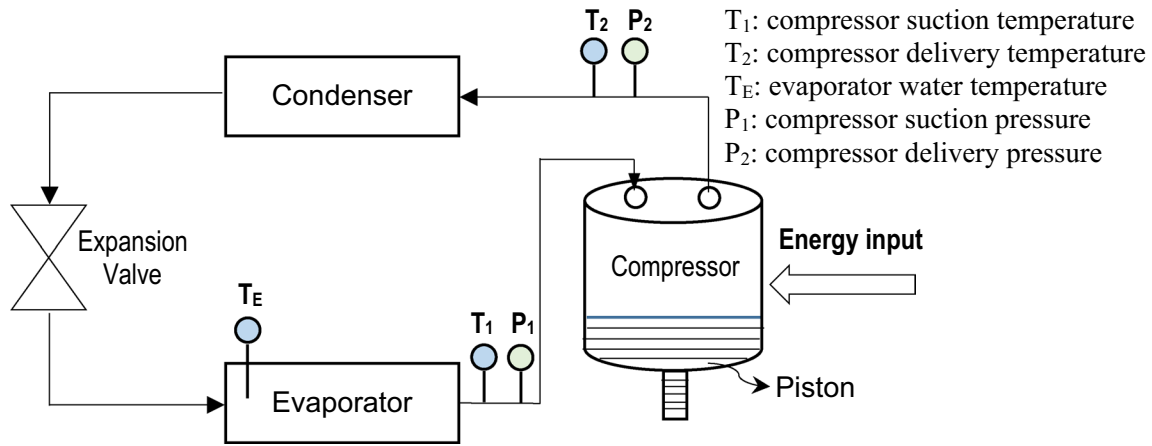
$$\text{SWR} = \frac{\Delta w}{\rho * L * F_N} \text{mm}^3 \text{N}^{-1} \text{m}^{-1} \tag{1}$$

Here Δw: wear weight loss of the pin during an experiment (g), ρ: density of the pin material (gcm^{-3}), F_N: applied load (N), and L: sliding distance covered (m).

Vapour compression refrigeration system testing

A VCRS test rig schematic diagram as shown in Fig. 7 was originally designed for R134a refrigerant and was used to perform VCRS experiments. It comprises four main components: a reciprocating HFC or an HC compressor (each having a horsepower of 1/5), an evaporator with a 13 L capacity equipped with cooling coils on its inner cylindrical wall, a forced-air condenser, and a capillary tube as an expansion device. Three different T-type thermocouples and two pressure gauges (bourdon-type) were used for the measurement of temperature and pressure at different locations. One thermocouple was positioned at the suction line of the compressor, a second at the delivery line of the compressor, and a third one to monitor the water temperature in the evaporator cabin. Similarly, pressure gauges were connected at the compressor's suction and delivery points. An analog static energy meter was employed to measure the compressor power consumption in both tests for each kind of compressor. The energy meter had a counting precision of 3200 impulse kW^{-1} h^{-1} (Sabareesh et al. 2012; Ravinder Kumar and Singh 2016; Yilmaz 2020). The compressor was disengaged from the rig after performing an experiment with one type of sample of the compressor lubricant. Subsequently, the compressor lubricant was replaced with the next sample of the compressor lubricant and was connected back to the test rig. Before connecting the compressor to the test rig, the VCRS underwent evacuation to remove moisture and foreign particles. This evacuation process involved running a vacuum pump for about three hours to ensure its effective performance (Sabareesh et al. 2012; Madyira et al. 2022; Gill et al. 2018). The parameters required for determining the compressor power consumption and the refrigeration effect were recorded carefully in each VCRS experiment. Each experiment involved running the VCR test rig for

T1: compressor suction temperature
T2: compressor delivery temperature
TE: evaporator water temperature
P1: compressor suction pressure
P2: compressor delivery pressure

Fig. 7 Schematic diagram of VCRS test rig

180 min, with readings taken at a regular interval of five minutes. The water temperature in the evaporator cabin was measured using a thermocouple, with a time interval '*t*' in between. The power consumption by the compressor was recorded by measuring the time (using a stopwatch) taken by the analog energy meter to register ten pulses. The complete set of readings was also collected in a similar manner by replacing the HFC compressor with the HC compressor.

Utilizing the standard Eqs. 2, 3, and 4, respectively (Sabareesh et al. 2012; Ravinder Kumar and Singh 2016; Yilmaz 2020), the refrigeration effect, power consumption by compressor, and COP of the VCRS were calculated based on the collected data under ambient temperatures ranging from 29 to 30 °C.

The uncertainty of each measuring instrument was assessed following the methodology detailed by Schultz. and Cole. (1979). In addition, the uncertainty linked to the specific parameter, such as Z, was determined by utilizing Eq. 5 (Ohunakin et al. 2017; Adelekan et al. 2021; Jatinder et al. 2019; Sanukrishna et al. 2019).

$$\text{Refrigeration effect} = \frac{m \times C_p \times \Delta T}{t} W \tag{2}$$

$$\text{Compressor power consumption} = \frac{n \times 3600}{t \times K} W \tag{3}$$

$$\text{COP} = \frac{\text{Refrigeration effect}}{\text{Compressor power consumption}} \tag{4}$$

$$U_z = \left[\sum_{i=1}^{n} \left(\frac{\partial z}{\partial p_i} U_{p_i} \right)^2 \right]^{0.5} \tag{5}$$

Equation 5 defines Z as the specific parameter, U_Z as the total uncertainty, U_{p_i} as the uncertainty linked to each independent variable, and n as the total number of variables. The acquired experimental uncertainties are shown in Table 3.

Results and discussion

Nanoparticles analysis (characterizations)

The FE-SEM image shown in Fig. 8 reveals a predominantly spherical shape of SiO_2 nanoparticles. Spherical nanoparticles in the base lubricant maintain their shape even at high temperatures and heavy loads, contributing to multiple mechanisms for reducing wear and friction between the rubbing surfaces (Lee et al. 2009; Muzammil S. Khan et al. 2019b). In addition, Xiaohao Wei et al. (2009) and Alawi et al. (2018) observed that nanoparticles with spherical morphology possessed higher thermal conductivity compared to other shapes. The images also show that these particles tend to clump together, forming agglomerations. Figure 9 shows the XRD patterns which confirmed the composition of SiO_2 nanoparticles. The XRD analysis also confirmed

Table 3 Uncertainty values of the different measured parameters of the experiment

S. No	Parameters	Uncertainty
1	Compressor suction pressure, P_1 (kPa)	± 1.12
2	Compressor discharge pressure, P_2 (kPa)	± 5.22
3	Compressor suction temperature, T_1 (℃)	± 0.10
4	Compressor discharge temperature, T_1 (℃)	± 0.22
5	Water temperature in evaporator cabin, T_w (℃)	± 0.12
6	Refrigeration effect (W)	± 0.52
7	Power consumption (W)	± 0.14
8	COP (%)	± 0.55
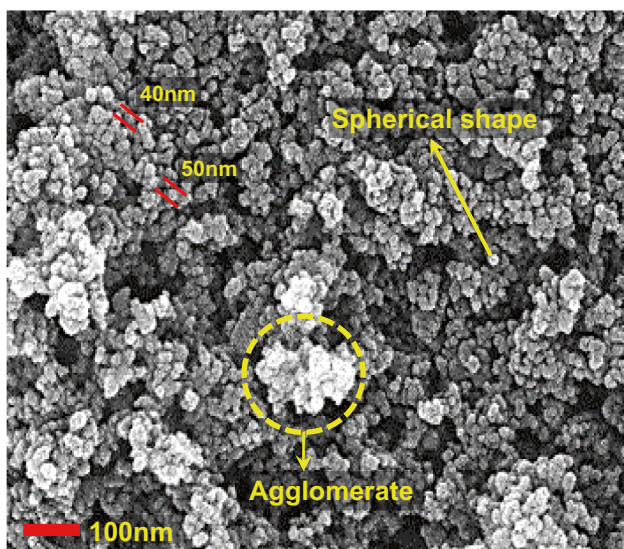
Fig. 8 FE-SEM images of SiO$_2$ nanoparticles

Fig. 10 FTIR spectrum of SiO$_2$ nanoparticles

Fig. 9 XRD of SiO$_2$ nanoparticles
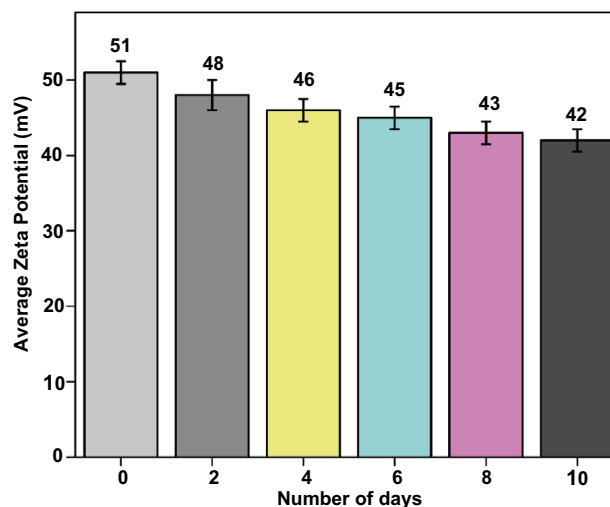
Fig. 11 Average Zeta potential values of sample K2 for distinct days
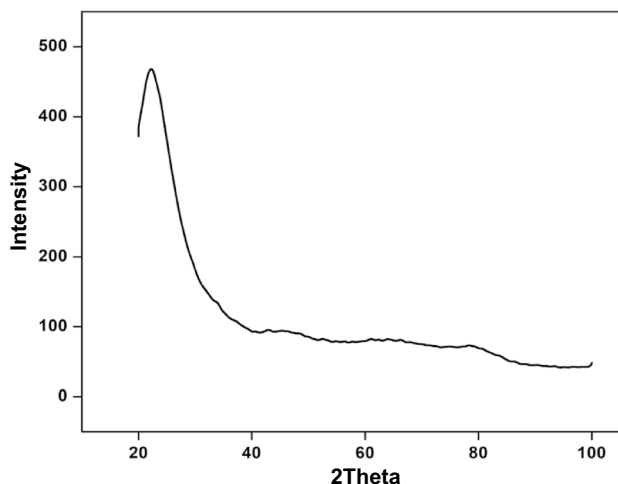
that particles of SiO$_2$ are in an amorphous state, lacking a crystalline structure (Tkachenko et al. 2020; Le Ba et al. 2020). Figure 10 shows the FTIR spectra related to SiO$_2$ nanoparticles. The broad diffraction peaks observed in FTIR spectra also confirms the amorphous nature of the used SiO$_2$ nanoparticles (Rawat et al. 2018).

Stability analysis

Figure 11 shows the average Zeta potential obtained for the prepared nanolubricant (sample K2) on different days. In general, the Zeta potential exceeding ± 30 mV indicates nanolubricant stability (Wu et al. 2009; Bakhtiari et al. 2021). The findings show that for each day, the
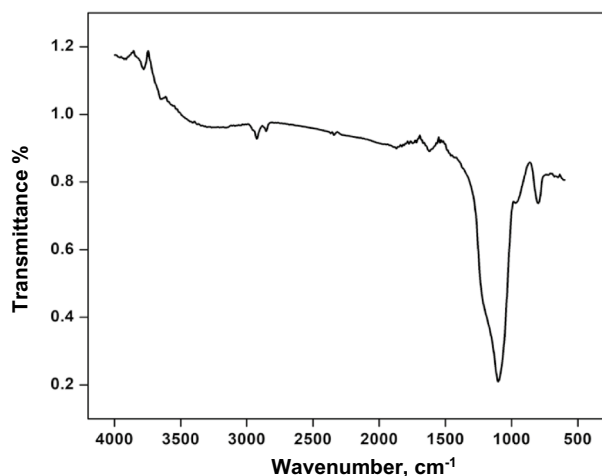
nanolubricant average Zeta potential exceeded 30 mV. This indicates that the SiO$_2$ nanoparticles were well distributed and the stability of their dispersion in compressor lubricant was satisfactory. The obtained results also indicate that the average Zeta potential of the lubricant sample K2 exhibited a slight decrease over the pre-decided time period of ten days. Comparable findings were also observed by Baojie. Wei et al. (2017).
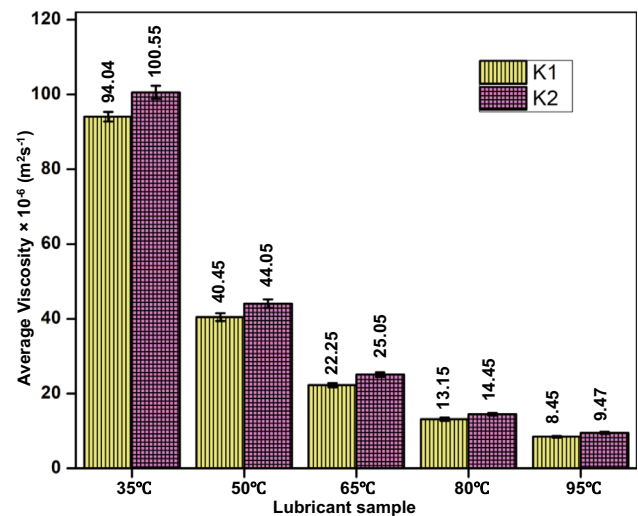
Thermal conductivity analysis

The bar graph in Fig. 12 shows that the average thermal conductivity of both lubricant samples decreased with the increase in temperature. The observed decline in average thermal conductivity is commonly ascribed to a reduction in molecular collisions. At higher temperatures, the mean
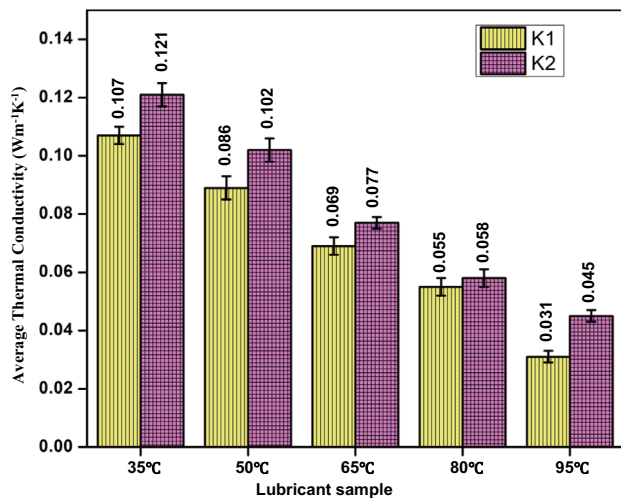
Fig. 12 Average thermal conductivity of POE oil and prepared nanolubricant at different temperatures

Fig. 13 Average viscosity of POE oil and prepared nanolubricant at different temperatures

path traversed by the molecules becomes longer, resulting in reduced opportunities for intermolecular interactions and, consequently, lower thermal conductivity (Sharif et al. 2016; Ravinder Kumar et al. 2020). The dispersion of nanoparticles improved the thermal conductivity of sample K1, as for each test temperature, the average thermal conductivity of sample K2 is more than that of sample K1. This could be due to the emergence of a micro-convection effect promoted by the nanoparticles dispersed in the sample K1 (Navdeep Kumar et al. 2023), and the development of layers of base lubricant on the surface of solid nanoparticles (Kotia et al. 2017).

However, this enhancement follows a discontinuous trend across the temperature range (35–95 °C). At 35 °C, sample K2 exhibits about a 13% increase in average thermal conductivity compared to sample K1. At 50 °C, this enhancement increases to about 19%, indicating the continued positive effect of the nanoparticles on heat conduction. However, at 65 °C, the enhancement decreases to about 12%, compared to sample K1, likely due to the formation of nanoparticle clusters that hinder efficient heat transfer. At 80 °C, the enhancement further reduces to about 6% than sample K1, as the temperature promotes a more significant clustering of nanoparticles. Interestingly, at 95 °C, sample K2 exhibits a substantial about 45% more thermal conductivity than sample K1, likely due to the breakdown of nanoparticle clusters and improved dispersion. The observed enhancement could be attributed to the aggressive motion (known as "Brownian motion") of the nanoparticles at elevated temperatures (Kotia et al. 2018; Yıldız et al. 2021; Wang et al. 2012; Li et al. 2021). A similar improvement in thermal conductivity for SiO_2 nanoparticles dispersed in POE oil was observed by Narayanasarma and Kuzhiveli (2019).

The thermal conductivity was significantly affected by the increase in temperature within the range of 35–95 °C, experiencing a reduction of about 70%. But on comparing the thermal conductivity of sample K1 at 35 °C and that of sample K2 at 95 °C, the reduction in thermal conductivity decreased from 70% to about 58%. Therefore, the effect of an increase in temperature from 35 to 95 °C on thermal conductivity was reduced by about 12% due to the dispersion of SiO_2 nanoparticles in POE oil.
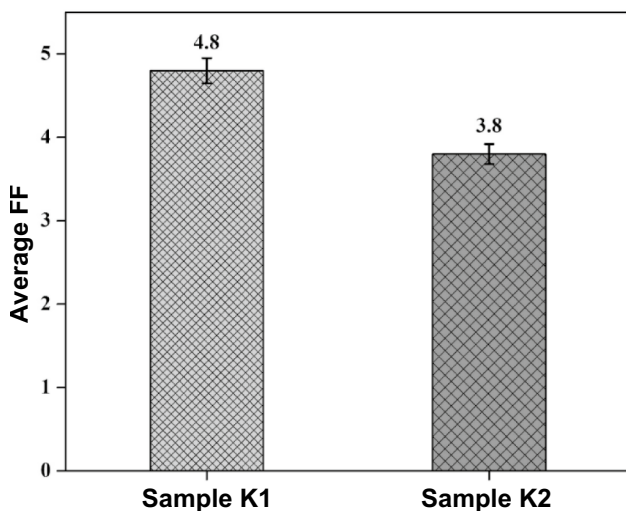
Viscosity analysis

The bar graphs (Fig. 13) show that at any of the test temperatures, sample K2 exhibits better average viscosity than sample K1. In general, viscosity decreases as temperature increases (Narayanasarma and Kuzhiveli 2019), and the bar graph follows a similar trend of variation in the viscosity of the respective lubricant sample with the temperature rise. However, as the temperature increases the reduction in average viscosity of each sample does not display a uniform trend.

At 35 °C, sample K2 shows about a 7% higher average viscosity than sample K1 due to SiO_2 nanoparticles dispersed in the base lubricant, slightly affecting its flow at lower temperatures. The nanoparticles may cause slight intermolecular interactions or hinder the movement of lubricant molecules, resulting in a slightly higher viscosity as observed by Kotia et al. (2017). However, at higher temperatures of 65 °C and 80 °C, the average viscosity of the nanolubricant initially increases and then decreases before increasing again at 95 °C. This behavior can be explained by the combined effects of nanoparticle dispersion and temperature. At 65 °C, the increase in average viscosity of
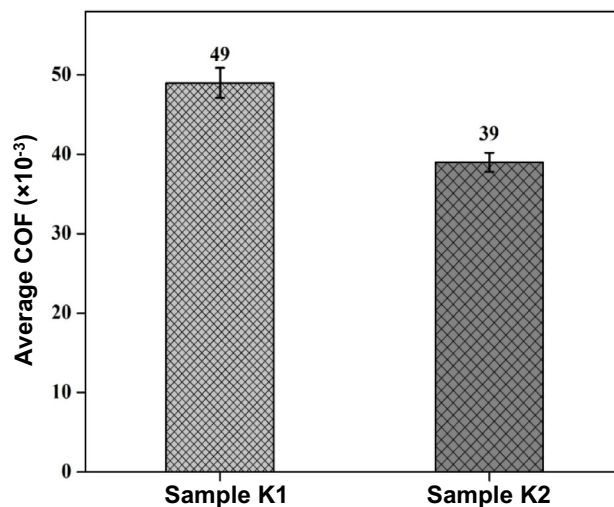
sample K2 is approximately 13% higher than that of sample K1. This significant enhancement may be ascribed to more intense movement and interactions between the molecules of the base lubricant and the dispersed nanoparticles at high temperatures. These interactions can cause the formation of temporary nanoparticle clusters or agglomerates, leading to a further increase in viscosity. At 80 °C, the average viscosity of sample K2 decreases slightly compared to temperature 65 °C. This decrease could be due to the increased thermal energy causing the partial breakdown of nanoparticle clusters or agglomerates, resulting in a reduction in viscosity. However, at 95 °C, the average viscosity of sample K2 again increases, showing approximately a 12% enhancement compared to sample K1. The elevated temperature increases thermal energy, outweighing the breakdown of nanoparticle clusters leading to a net increase in viscosity. Therefore, the rise in the viscosity of the nanolubricant may be attributed to the dispersion of nanoparticles (SiO_2) in the base lubricant (Sanukrishna et al. 2018; Narayanasarma and Kuzhiveli 2019).

Coefficient of friction and specific wear rate analysis

The pin-on-disc tribometer tester results show that the nanolubricant reduced both FF (measured in N, see Fig. 14) and wear (measured in µm) compared to base lubricant. The results revealed that under controlled test conditions, the calculated average COF value between the mating surfaces with sample K2 was more than 20% lower than that with the sample K1 (Fig. 15). Similarly, the average SWR for the sample K2 was nearly 29% lower as compared to that of the sample K1 (see Fig. 16).
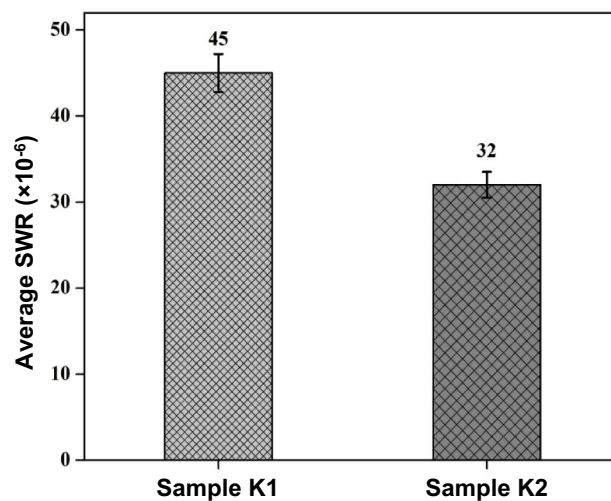

Fig. 15 Average COF of POE oil and prepared nanolubricant during pin-on-disc tribometer wear test

The mechanisms behind the enhancement of wear and friction reduction characteristics of sample K2 can be categorized into two distinct groups. The first mechanism is attributed to the direct impact of nanoparticles, specifically the rolling effect and formation of tribo-film (Rapoport et al. 2002; Xu et al. 1996; Singh et al. 2020; Sanukrishna et al. 2019). The secondary mechanism includes polishing and mending effects (Tang and Li 2014; Rawat et al. 2018; Sanukrishna et al. 2019). The friction between the mating pair can be reduced by minimizing the contact between the mating surfaces and reducing surface roughness (Yilmaz 2020). The spherical morphology of nanoparticles offers the benefit of the rolling effect which minimizes the sliding

Fig. 14 Average FF of POE oil and prepared nanolubricant during pin-on-disc tribometer wear test


Fig. 16 Average SWR of POE oil and prepared nanolubricant during pin-on-disc tribometer wear test

contact between the mating surfaces (Ge et al. 2015; Rawat et al. 2018; Patil et al. 2013a). The self-repairing (mending effect) and polishing effect minimize the surface roughness and abrasive wear on the mating surfaces (Sanukrishna et al. 2019; Ge et al. 2015). At higher temperatures, the formation of tribo-film due to nanolubricant provides the additional benefit of protecting the surfaces and reducing friction and wear between them (Sanukrishna et al. 2019). The nanoparticles within the base lubricant also serve as a third body and reduce severe wear (Abdel-Rehim et al. 2021). The discussed mechanisms are shown in the schematic diagram in Fig. 17. The morphology and size of the SiO_2 nanoparticles along with the observed reduced SWR, witness the expressed mechanism.

The current research findings show a decrease in the average COF when SiO_2 nanoparticles were added to the base lubricant, as observed by Hamisa et al. (2023), Rawat et al. (2018), and Sanukrishna et al. (2019). Moreover, this research revealed better result of average COF (6% more) as compared to that reported by Hamisa et al. (2023), used the same ratio of SiO_2 nanoparticles (0.1 gL^{-1}) in POE oil. In addition, SiO_2 nanoparticles based lubricant reduced wear between the mating surfaces, as also observed by S. S. Sanukrishna et al. (2019) and Rawat et al. (2018).

Refrigeration effect

The comparison of the average refrigeration effect between the retrofitted and HC compressor based VCRS using HC refrigerant R600a, as determined with lubricant samples K1 and K2, can be clearly seen in a bar graph (Fig. 18). The results show that the average refrigeration effect for each compressor type improved significantly with the utilization of a compressor lubricant containing SiO_2 nanoparticles. This improvement might be due to the circulating refrigerant
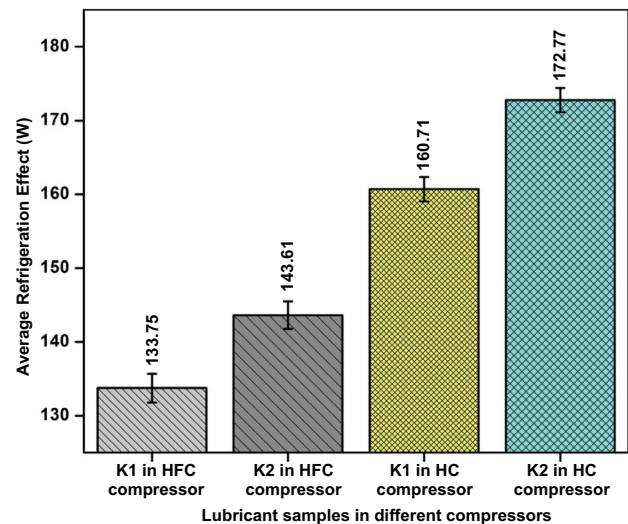
Fig. 18 Average refrigeration effect of VCRS using different lubricant samples in different compressors

carrying traces of nanolubricants during functioning, reaching the evaporating cabin and other parts of the VCRS, acting as a nanolubricant-refrigerant mixture (Narayanasarma and Kuzhiveli 2019; Sanukrishna et al. 2019). For each compressor, the SiO_2 nanoparticles within the sample K1 resulted in about 7% enhancement in the average refrigeration effect. But on comparing the average refrigeration effect of sample K2 in the HC compressor with that of sample K1 in the HFC compressor an improvement of about 29% is observed. In addition, the HC compressor, without using nanoparticles, performed even better as compared to the nanolubricant used in the retrofitted VCRS. The bar graph shows about 12% enhancement of the average refrigeration effect with sample K1 in HC compressor based VCRS

Fig. 17 Schematic representation of various mechanisms involved in friction and wear reduction between the mating surfaces
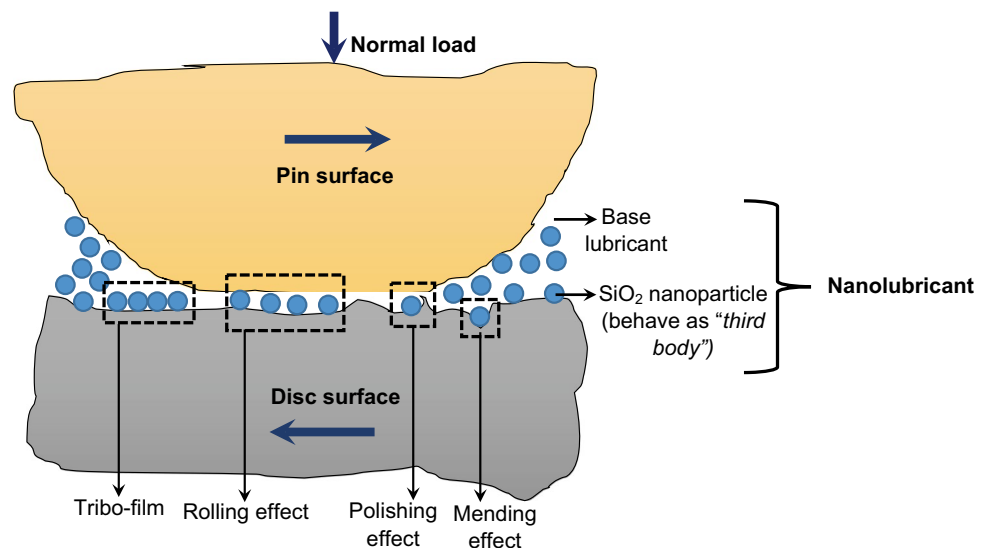
compared to sample K2 in HFC compressor based retrofitted VCRS.

Power consumption

It is observed from the bar graph shown in Fig. 19 that the average power consumption by each compressor reduced when nanolubricant was used instead of the base lubricant. For the retrofitted system, nearly 3% reduction is observed with the use of nanolubricant instead of the base lubricant. However, the results also reveal that the VCRS with nanolubricant and an HC compressor consumed more than 7% less average power compared to that in the retrofitted system filled with the POE oil. Without considering the role of nanoparticles, the use of only an HC compressor instead of retrofitting in an HFC compressor resulted in more than 4% less power consumption.

Retrofitting offers the convenience of using the same device while switching to an eco-friendly HC refrigerant. However, the observed difference in power consumption suggests that prolonged use may result in an overall economic loss. This is because the cost of replacing the compressor becomes less as compared to the increased energy input during its operation. Furthermore, this higher energy consumption also has a negative impact on the environment. Therefore, switching to an HC compressor designed for eco-friendly HC refrigerants may lead to overall savings in power consumption and a positive environmental impact.

In either compressor, the role of SiO_2 nanoparticles dispersed into the POE oil (forming a nanolubricant) can be well understood in reducing power consumption by nearly 3%. The role of nanoparticles is even more significant in

reducing the power consumption by 3.38% in the case of the HC compressor. As observed in the FE-SEM micrograph (Fig. 8), the spherical shape of nano-sized SiO_2 particles dispersed in POE oil might have played a substantial role in the observed drop-in power consumption. The spherical shape offers a rolling effect and the SiO_2 particles behave as nano-ball bearings to reduce the power loss due to reduction in friction between the mating surfaces (Sanukrishna et al. 2019). The nano-sized SiO_2 particles also offer mending and polishing effect, by filling the micro-grooves and breaking the surface asperities, respectively (Rawat et al. 2018; Yilmaz 2020). The higher viscosity of the nanolubricant (Fig. 13) further assists in developing a consistent tribo-film on the surfaces of piston-cylinder mating, leading to a substantial reduction in power loss due to friction. About more than 20% reduction in both the average FF and the average COF, as observed in the wear test, clearly evidenced the drop-in power consumption with sample K2 in either of the compressors. In the wear test, about 30% drop in the average SWR for sample K2 as compared to sample K1 also witnessed the proposed mechanisms (Fig. 17), which are also motivated by previous literature (Rawat et al. 2018; Singh et al. 2020). A smaller amount of frictional heat is expected to be produced in the compressor due to less average FF (about 20% less with nanolubricant, Fig. 14). Considering the thermodynamics aspects of the compression a more frictional heat leads to an increased compressor work due to the addition of extra flow work (Moran et al. 2018). The frictional heat increases the volume of the refrigerant vapors and therefore compressor demands more power to handle the increased volume of the refrigerant vapors (Whitman et al. 2012). The increased temperature after compression also affects the refrigeration effect in the next part of the VCRS cycle, as already observed in Fig. 18.

Surprisingly, during this research, VCRS equipped with an HC compressor using sample K1, consumed even less average power than the retrofitted system filled with sample K2. This could be attributed to the better compatibility between the HC-based compressor, the HC R600a refrigerant, and each component of the VCRS. The power reduction, resulting from the use of an HC compressor in the VCRS, as compared to the retrofitted system, was also observed by Rasti et al. (2013).

Coefficient of performance

The average COP of the VCRS obtained using each kind of compressor with each kind of compressor lubricant sample can be compared easily from the bar graph (Fig. 20). As the COP is obtained from the refrigeration effect and power consumption, the trend of the COP is purely in alignment with the results discussed for refrigeration effect and the power consumption. A remarkable increase of about 25% in average COP can be
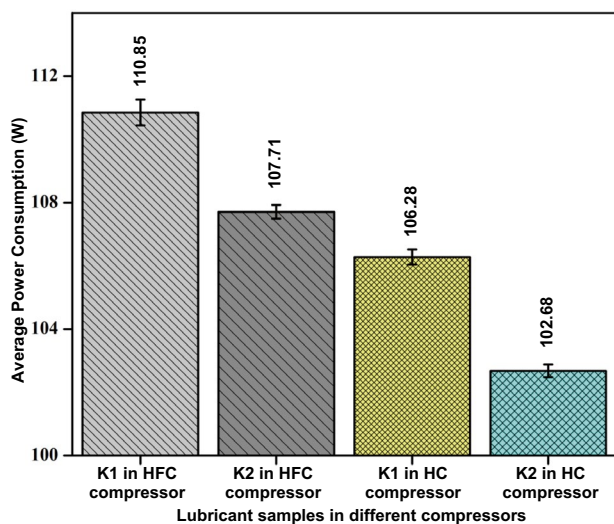
Fig. 19 Average power consumption by VCRS using different compressor lubricant samples in different compressors
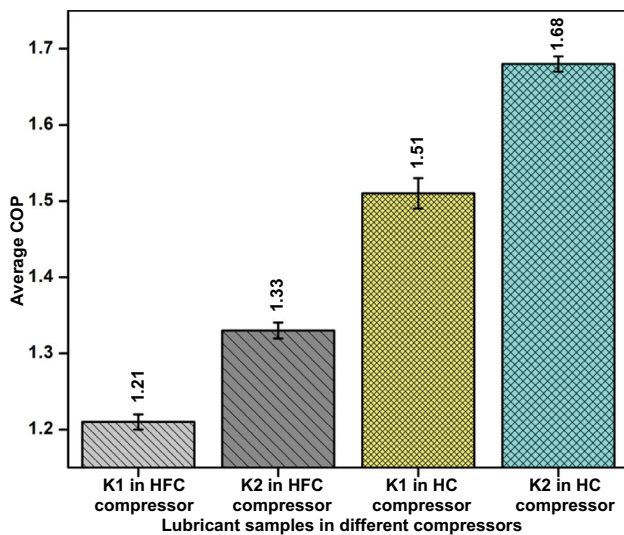
Fig. 20 Average COP of the VCRS using different lubricant samples in different compressors

seen with the HC compressor as compared to that with the retrofitted HFC compressor, for the respective lubricant samples used. While considering the effect of the compressor lubricant sample, an increase of about 10% can be discerned with the respective compressor for sample K2 as compared to the lubricant sample K1. The contribution of dispersed nanoparticles in the base lubricant has been discussed thoroughly in the refrigeration effect and power-consumption sections. As this about 7% increase in average refrigeration effect and about 3% decrease in average power consumption has jointly resulted in an about 10% increase in average COP. On the other hand, as already discussed, switching from HFC to HC compressor has resulted into a bigger change in power consumption and refrigeration effect combine resulted into about 25% hike in average COP. On comparing the performance of sample K1 with the HFC compressor with that of sample K2 with the HC compressor, about 39% hike in average COP is already visible in the bar graph (Fig. 20).

When comparing the performance of sample K1 with the HFC compressor to that of sample K2 with the HC compressor, a significant 39% increase in the average COP is already evident in the bar graph (Fig. 20). The present research with HC compressor shows better results of average COP than Ohunakin et al. (2018). The authors also used SiO_2 nanoparticles with HC refrigerant in the retrofitted VCRS.

Conclusions

In this research, the role of SiO_2 nanoparticles in compressor lubricant POE oil used in a retrofitted and an HC compressor based VCRS are investigated. Using eco-friendly

HC R600a refrigerant, the performance characteristics including power consumption by compressor, refrigeration effect, and COP were compared for the base lubricant and the prepared nanolubricant used in the VCRS compressor. The present research leads to the following conclusions:

- The dispersion of nanoparticles into POE oil improved its thermophysical and tribological characteristics, such as thermal conductivity and viscosity, even at higher temperatures. The use of nanolubricant resulted in lower weight loss in pin-on-disc wear testing with the pin made from actual compressor material and indicated the benefits obtained through the improved tribological and thermophysical properties. As compared to POE oil, the use of SiO_2 nanoparticles based nanolubricant as the compressor lubricant, resulted in about 7% higher power savings, when used in either of the retrofitted VCRS and also that using HC-based compressor.
- The power saving and the overall enhancement in the performance of each type of VCRS can be attributed to multiple mechanisms, including the polishing, rolling, and mending effects, and the development of tribo-film between the mating surfaces, enabled by nano-sized SiO_2 nanoparticles.
- The nanolubricant-filled HC compressor based VCRS exhibited better performance than the nanolubricant-filled retrofitted VCRS. It indicated better compatibility of nanolubricant with the used HC refrigerant R600a and the HC-based compressor.
- Comparatively lower temperatures achieved after compression due to reduced friction offered by nanolubricant in either of the compressors, also resulted in a higher refrigeration effect in the evaporator. Both contributors, higher refrigeration effect along with reduced power consumption, resulted in a higher COP.

The better performance of an HC compressor based VCRS compared to a retrofitted VCRS using HC refrigerant R600a shows that the flexibility of retrofitting for the long run is not economically viable. The power consumption associated with retrofitting may exceed the cost of replacing the compressor. Therefore, it is recommended to switch from HFC to an HC compressor using HC refrigerant R600a to improve the performance of the VCRS.

Compliance with ethical standards

Conflict of interest On behalf of all authors, the corresponding author states that there is no conflict of interest.

References

Abdel-Hadi EA, Taher SH, Abdelrahman HE, Ahmed HM, Mustafa SA (2016) Experimental investigation of flow-boiling heat transfer using nano-refrigerant. J Eng Appl Sci 63:335–353

Abdel-Rehim AA, Akl S, Elsoudy S (2021) Investigation of the tribological behavior of mineral lubricant using copper oxide nano additives. Lubricants 9(2):16. https://doi.org/10.3390/lubricants 9020016

Adelekan DS, Ohunakin OS, Gill J, Atiba OE, Okokpujie IP, Atayero AA (2019a) Experimental investigation of vapour compression system with 15nm TiO2-R600a nano-refrigerant as the working fluid. Procedia Manuf 35:1222–1227

Adelekan DS, Ohunakin OS, Gill J, Atiba OE, Okokpujie IP, Atayero AA (2019b) Performance of a domestic refrigerator infused with safe charge of R600a refrigerant and various concentrations of TiO2 nanolubricant. Procedia Manuf 35:1158–1164

Adelekan DS, Ohunakin OS, Oladeinde MH, Jatinder G, Atiba OE, Nkiko MO et al (2021) Performance of a domestic refrigerator in varying ambient temperatures, concentrations of TiO2 nanolubricants and R600a refrigerant charges. Heliyon 7(2):e06156. https://doi.org/10.1016/j.heliyon.2021.e06156

Akhavan-Behabadi MA, Sadoughi MK, Darzi M, Fakoor-Pakdaman M (2015) Experimental study on heat transfer characteristics of R600a/POE/CuO nano-refrigerant flow condensation. Exp Thermal Fluid Sci 66:46–52. https://doi.org/10.1016/j.expthermflusci.2015.02.027

Alawi OA, Sidik NAC, Xian HW, Kean TH, Kazi SN (2018) Thermal conductivity and viscosity models of metallic oxides nanofluids. Int J Heat Mass Transf 116:1314–1325. https://doi.org/10.1016/j.ijheatmasstransfer.2017.09.133

Asadi A, Alarifi IM, Ali V, Nguyen HM (2019) An experimental investigation on the effects of ultrasonication time on stability and thermal conductivity of MWCNT-water nanofluid: finding the optimum ultrasonication time. Ultrason Sonochem 58:104639. https://doi.org/10.1016/j.ultsonch.2019.104639

Babarinde TO, Akinlabi SA, Madyira DM (2019) Experimental investigation of R600a/TiO2/mineral oil as a drop-in replacement for R134a/POE oil in a household refrigeration system. Int J Ambient Energy. https://doi.org/10.1080/01430750.2019.1653983

Babarinde TO, Akinlabib SA, Madyiraa DM, Ekundayod FM (2020) Enhancing the energy efficiency of vapour compression refrigerator system using R600a with graphene nanolubricant. Energy Rep 6:1–10. https://doi.org/10.1016/j.egyr.2019.11.031

Bakhtiari R, Kamkari B, Afrand M, Abdollahi A (2021) Preparation of stable TiO2-graphene/water hybrid nanofluids and development of a new correlation for thermal conductivity. Powder Technol 385:466–477. https://doi.org/10.1016/j.powtec.2021.03.010

Bi S, Guo K, Liu Z, Wu J (2011) Performance of a domestic refrigerator using TiO2-R600a nano-refrigerant as working fluid. Energy Convers Manag 52(1):733–737. https://doi.org/10.1016/j.enconman.2010.07.052

Borode AO, Ahmed NA, Olubambi PA (2019) A review of heat transfer application of carbon-based nanofluid in heat exchangers. NanoStruct Nano-Objects 20:1–20. https://doi.org/10.1016/j.nanoso.2019.100394

Cao X, Wang X, Song Q, Wang D, Li Y (2021) Experimental investigation on the heat transfer and pressure drop characteristics of R600a in a minichannel condenser with different inclined angles. Appl Therm Eng. https://doi.org/10.1016/j.applthermaleng.2021.117227

Chakraborty S, Panigrahi PK (2020) Stability of nanofluid: a review. Appl Therm Eng 174:126. https://doi.org/10.1016/j.applthermaleng.2020.115259

Chauhan SS, Kumar R, Rajput SPS (2019) Performance investigation of ice plant working with R134a and different concentrations of POE/TiO2 nanolubricant using experimental method. J Braz Soc Mech Sci Eng 41(4):1–10. https://doi.org/10.1007/s40430-019-1657-3

Devendiran DK, Amirtham VA (2016) A review on preparation, characterization, properties and applications of nanofluids. Renew Sustain Energy Rev 60:21–40. https://doi.org/10.1016/j.rser.2016.01.055

Fatouh M, Abou-Ziyan H (2018) Energy and exergy analysis of a household refrigerator using a ternary hydrocarbon mixture in tropical environment: effects of refrigerant charge and capillary length. Appl Therm Eng 145:14–26. https://doi.org/10.1016/j.applthermaleng.2018.09.008

Ge X, Xia Y, Cao Z (2015) Tribological properties and insulation effect of nanometer TiO2 and nanometer SiO2 as additives in grease. Tribol Int 92:454–461. https://doi.org/10.1016/j.triboint.2015.07.031

Ghorbani B, Akhavan-Behabadi MA, Ebrahimi S, Vijayaraghavan K (2017) Experimental investigation of condensation heat transfer of R600a/POE/CuO nano-refrigerant in flattened tubes. Int Commun Heat Mass Transf 88:236–244. https://doi.org/10.1016/j.icheatmasstransfer.2017.09.011

Gill J, Singh J, Ohunakin OS, Adelekan DS (2018) Artificial neural network approach for irreversibility performance analysis of domestic refrigerator by utilizing LPG with TiO2–lubricant as replacement of R134a. Int J Refrig 89:159–176. https://doi.org/10.1016/j.ijrefrig.2018.02.025

Goto M, Honda F (2004) Film-thickness effect of Ag lubricant layer in the nano-region. Wear 256(11–12):1062–1071. https://doi.org/10.1016/s0043-1648(03)00530-1

Gupta M, Kumar R, Arora N, Kumar S, Dilbagi N (2015) Forced convective heat transfer of MWCNT/water nanofluid under constant heat flux: an experimental investigation. Arab J Sci Eng 41(2):599–609. https://doi.org/10.1007/s13369-015-1699-5

Gupta M, Singh V, Kumar S, Dilbaghi N (2020) Experimental analysis of heat transfer behavior of silver, MWCNT and hybrid (silver+MWCNT) nanofluids in a laminar tubular flow. J Therm Anal Calorim 142(4):1545–1559. https://doi.org/10.1007/s10973-020-09453-w

Hamid KA, Azmi WH, Nabil MF, Mamat R, Sharma KV (2018) Experimental investigation of thermal conductivity and dynamic viscosity on nanoparticle mixture ratios of TiO2-SiO2 nanofluids. Int J Heat Mass Transf 116:1143–1152. https://doi.org/10.1016/j.ijheatmasstransfer.2017.09.087

Hamisa AH, Azmi WH, Ismail MF, Rahim RA, Ali HM (2023) Tribology performance of polyol-ester based TiO2, SiO2, and their hybrid nanolubricants. Lubricants 11(1):18. https://doi.org/10.3390/lubricants11010018

Harby K (2017) Hydrocarbons and their mixtures as alternatives to environmental unfriendly halogenated refrigerants: an updated overview. Renew Sustain Energy Rev 73:1247–1264. https://doi.org/10.1016/j.rser.2017.02.039

Hatami M, Jing D (2020) Introduction to nanofluids. nanofluids. Elsevier, pp 1–50. https://doi.org/10.1016/b978-0-08-102933-6.00001-9

Ingole S, Charanpahari A, Kakade A, Umare SS, Bhatt DV, Menghani J (2013) Tribological behavior of nano TiO2 as an additive in base oil. Wear 301(1–2):776–785. https://doi.org/10.1016/j.wear.2013.01.037

Jatinder G, Ohunakin OS, Adelekan DS, Atiba OE, Daniel AB, Singh J et al (2019) Performance of a domestic refrigerator using selected

hydrocarbon working fluids and TiO$_2$–MO nanolubricant. Appl Therm Eng. https://doi.org/10.1016/j.applthermaleng.2019.114004

Kaggwa A, Carson JK (2019) Developments and future insights of using nanofluids for heat transfer enhancements in thermal systems: a review of recent literature. Int Nano Lett 9(4):277–288. https://doi.org/10.1007/s40089-019-00281-x

Khan I, Saeed K, Khan I (2019a) Nanoparticles: properties, applications and toxicities. Arab J Chem 12(7):908–931. https://doi.org/10.1016/j.arabjc.2017.05.011

Khan MS, Sisodia MS, Gupta S, Feroskhan M, Kannan S, Krishnasamy K (2019b) Measurement of tribological properties of Cu and Ag blended coconut oil nanofluids for metal cutting. Eng Sci Technol, Int J 22(6):1187–1192. https://doi.org/10.1016/j.jestch.2019.04.005

Kong L, Zhang L, Bao Y, Liu D, Liu S, Zang Z (2022) Effect of surface roughness and particle size on lubrication mechanisms of SiO$_2$ nanoparticles. Adv Mater Sci Eng 2022:1–11. https://doi.org/10.1155/2022/7051650

Kotia A, Borkakoti S, Deval P, Ghosh SK (2017) Review of interfacial layer's effect on thermal conductivity in nanofluid. Heat Mass Transf 53(6):2199–2209. https://doi.org/10.1007/s00231-016-1963-6

Kotia A, Rajkhowa P, Rao GS, Ghosh SK (2018) Thermophysical and tribological properties of nanolubricants: a review. Heat Mass Transf 54(11):3493–3508. https://doi.org/10.1007/s00231-018-2351-1

Kotia A, Ghosh GK, Srivastava I, Deval P, Ghosh SK (2019) Mechanism for improvement of friction/wear by using Al$_2$O$_3$ and SiO$_2$/Gear oil nanolubricants. J Alloy Compd 782:592–599. https://doi.org/10.1016/j.jallcom.2018.12.215

Kumar R, Singh J (2016) Effect of ZnO nanoparticles in R290/R600a (50/50) based vapour compression refrigeration system added via lubricant oil on compressor suction and discharge characteristics. Heat Mass Transf 53(5):1579–1587. https://doi.org/10.1007/s00231-016-1921-3

Kumar A, Kumar P, Singh B (2021) Optimizing the effect of wear test parameters on the specific wear rate of AZ91D magnesium alloy. Mater Today Proc 44:4885–4890. https://doi.org/10.1016/j.matpr.2020.11.709

Kumar R, Singh DK, Chander S (2020) An experimental approach to study thermal and tribology behavior of LPG refrigerant and MO lubricant appended with ZnO nanoparticles in domestic refrigeration cycle. Heat Mass Transf 56(7):2303–2311. https://doi.org/10.1007/s00231-020-02860-7

Kumar R, Singh DK, Chander S (2022) A critical review on the effect of nanorefrigerant and nanolubricant on the performance of heat transfer cycles. Heat Mass Transf 58(9):1507–1531. https://doi.org/10.1007/s00231-022-03194-2

Kumar N, Kumar P, Goyal K (2023) A novel approach of using TiO$_2$ and SiO$_2$ nanoparticles and hydrocarbon refrigerant R600a in retrofitted vapour compression refrigeration system for environment protection and system performance enhancement. Appl Nanosci. https://doi.org/10.1007/s13204-023-02897-0

Laad M, Jatti VKS (2018) Titanium oxide nanoparticles as additives in engine oil. J King Saud Univ: Eng Sci 30(2):116–122. https://doi.org/10.1016/j.jksues.2016.01.008

Le Ba T, Várady ZI, Lukács IE, Molnár J, Balczár IA, Wongwises S et al (2020) Experimental investigation of rheological properties and thermal conductivity of SiO$_2$–P25 TiO$_2$ hybrid nanofluids. J Therm Anal Calorim 146(1):493–507. https://doi.org/10.1007/s10973-020-10022-4

Lee C-G, Hwang Y-J, Choi Y-M, Lee J-K, Choi C, Oh M (2009) A study on the tribological characteristics of graphite nano lubricants. Int J Precis Eng Manuf 10:85–90. https://doi.org/10.1007/s12541-009-0013-4

Li J, Zhang X, Xu B, Yuan M (2021) Nanofluid research and applications: a review. Int Commun Heat Mass Transf. https://doi.org/10.1016/j.icheatmasstransfer.2021.105543

Madyira DM, Babarinde TO, Mashinini PM (2022) Performance improvement of R600a with graphene nanolubricant in a domestic refrigerator as a potential substitute for R134a. Fuel Communications 10:1–8. https://doi.org/10.1016/j.jfueco.2021.100034

Mansourian R, Mousavi SM, Michaelides EE (2020) Improving the thermo-physical and rheological properties of crude oil (CO) by the synthesized CuO/SiO$_2$/CaP nanocomposite for drag reduction through horizontal pipelines. Appl Nanosci 11(2):347–362. https://doi.org/10.1007/s13204-020-01597-3

Moran MJ, Spapiro HN, Boettner DD, Bailey MB (2018) Fundamentals of engineering thermodynamics. Wiley

Nair V, Parekh AD, Tailor PR (2020) Experimental investigation of a vapour compression refrigeration system using R134a/nano-oil mixture. Int J Refrig 112:21–36. https://doi.org/10.1016/j.ijrefrig.2019.12.009

Narayanasrma S, Kuzhiveli BT (2019) Evaluation of the properties of POE/SiO$_2$ nanolubricant for an energy-efficient refrigeration system–an experimental assessment. Powder Technol 356:1029–1044. https://doi.org/10.1016/j.powtec.2019.09.024

Ohunakin OS, Adelekan DS, Babarinde TO, Leramo RO, Abam FI, Diarra CD (2017) Experimental investigation of TiO$_2$-, SiO$_2$- and Al$_2$O$_3$-lubricants for a domestic refrigerator system using LPG as working fluid. Appl Therm Eng 127:1469–1477. https://doi.org/10.1016/j.applthermaleng.2017.08.153

Ohunakin OS, Adelekan DS, Gill J, Atayero AA, Atiba OE, Okokpujie IP et al (2018) Performance of a hydrocarbon driven domestic refrigerator based on varying concentration of SiO$_2$ nano-lubricant. Int J Refrig 94:59–70. https://doi.org/10.1016/j.ijrefrig.2018.07.022

Okonkwo EC, Wole-Osho I, Almanassra IW, Abdullatif YM, Al-Ansari T (2020) An updated review of nanofluids in various heat transfer devices. J Therm Anal Calorim 145(6):2817–2872. https://doi.org/10.1007/s10973-020-09760-2

Padmanabhan VMV, Palanisamy S (2012) The use of TiO$_2$ nanoparticles to reduce refrigerator ir-reversibility. Energy Convers Manag 59:122–132. https://doi.org/10.1016/j.enconman.2012.03.002

Patil H, Chavan D, Pise AT (2013a) Tribological properties of SiO$_2$ nanoparticles added in SN-500 base oil. Int J Eng Res Technol (IJERT) 2(5):763–768

Rapoport L, Leshchinsky V, Lvovsky M, Nepomnyashchy O, Volovik Y, Tenne R (2002) Mechanism of friction of fullerenes. Ind Lubr Tribol 54(4):171–176. https://doi.org/10.1108/00368790210431727

Rasti M, Aghamiri S, Hatamipour M-S (2013) Energy efficiency enhancement of a domestic refrigerator using R436A and R600a as alternative refrigerants to R134a. Int J Therm Sci 74:86–94. https://doi.org/10.1016/j.ijthermalsci.2013.07.009

Rawat SS, Harsha AP, Deepak AP (2018) Tribological performance of paraffin grease with silica nanoparticles as an additive. Appl Nanosci 9(3):305–315. https://doi.org/10.1007/s13204-018-0911-9

Robertson J (2004) High dielectric constant oxides. The Eur Phys J Appl Phys 28(3):265–291. https://doi.org/10.1051/epjap:2004206

Sabareesh RK, Gobinath N, Sajith V, Das S, Sobhan CB (2012) Application of TiO$_2$ nanoparticles as a lubricant-additive for vapor compression refrigeration systems -an experimental investigation. Int J Refrig 35:1989–1996. https://doi.org/10.1016/j.ijrefrig.2012.07.002

Sanukrishna SS, Prakash MJ (2018) Experimental studies on thermal and rheological behaviour of TiO$_2$-PAG nanolubricant for refrigeration system. Int J Refrig 86:356–372. https://doi.org/10.1016/j.ijrefrig.2017.11.014

Sanukrishna SS, Vishnu S, Krishnakumar TS, Jose Prakash M (2018) Effect of oxide nanoparticles on the thermal, rheological and tribological behaviours of refrigerant compressor oil: an experimental investigation. Int J Refrig 90:32–45. https://doi.org/10.1016/j.ijrefrig.2018.04.006

Sanukrishna SS, Shafi M, Murukan M, Jose Prakash M (2019) Effect of SiO_2 nanoparticles on the heat transfer characteristics of refrigerant and tribological behaviour of lubricant. Powder Technol 356:39–49. https://doi.org/10.1016/j.powtec.2019.07.083

Schultz R, Cole R (1979) 'Uncertainty analysis in boiling nucleation.' In: AICHE symposium series. pp 32–39

Sharif MZ, Azmi WH, Redhwan AAM, Mamat R (2016) Investigation of thermal conductivity and viscosity of Al_2O_3/PAG nanolubricant for application in automotive air conditioning system. Int J Refrig 70:93–102. https://doi.org/10.1016/j.ijrefrig.2016.06.025

Sharif MZ, Azmia WH, Mamata R, Shaifuld AIM (2018) Mechanism for improvement in refrigeration system performance by using nanorefrigerants and nanolubricants: a review. Int Commun Heat Mass Transf. https://doi.org/10.1016/j.icheatmasstransfer.2018.02.012

Sia SY, Bassyony EZ, Sarhan AAD (2014) Development of SiO_2 nanolubrication system to be used in sliding bearings. Int J Adv Manuf Technol 71(5–8):1277–1284. https://doi.org/10.1007/s00170-013-5566-9

Sidik NAC, Mohammed HA, Alawi OA, Samion S (2014) A review on preparation methods and challenges of nanofluids. Int Commun Heat Mass Transf 54:115–125. https://doi.org/10.1016/j.icheatmasstransfer.2014.03.002

Singh A, Chauhan P, Mamatha TG (2020) A review on tribological performance of lubricants with nanoparticles additives. Mater Today: Proc 25:586–591. https://doi.org/10.1016/j.matpr.2019.07.245

Soliman AMA, Abdel Rahman AK, Ookawara S (2018) Enhancement of vapor compression cycle performance using nanofluids. J Therm Anal Calorim 135(2):1507–1520. https://doi.org/10.1007/s10973-018-7623-y

Tang Z, Li S (2014) A review of recent developments of friction modifiers for liquid lubricants (2007–present). Curr Opin Solid State Mater Sci 18(3):119–139. https://doi.org/10.1016/j.cossms.2014.02.002

Tkachenko T, Yevdokymenko V, Kamenskyh D, Sheludko Y, Povazhnyi V, Kashkovskyi V (2020) Physico-chemical properties of biogenic SiO_2 nanoparticles obtained from agriculture residue. Appl Nanosci 10(12):4617–4623. https://doi.org/10.1007/s13204-020-01383-1

Wang JJ, Zheng RT, Gao JW, Chen G (2012) Heat conduction mechanisms in nanofluids and suspensions. Nano Today 7(2):124–136. https://doi.org/10.1016/j.nantod.2012.02.007

Wei X, Zhu H, Kong T, Wang L (2009) Synthesis and thermal conductivity of Cu_2O nanofluids. Int J Heat Mass Transf 52(19–20):4371–4374. https://doi.org/10.1016/j.ijheatmasstransfer.2009.03.073

Wei B, Zou C, Li X (2017) Experimental investigation on stability and thermal conductivity of diathermic oil based TiO_2 nanofluids. Int J Heat Mass Transf 104:537–543. https://doi.org/10.1016/j.ijheatmasstransfer.2016.08.078

Whitman B, Johnson B, Tomczyk J, Silberstein E (2012) Refrigeration and air conditioning technology. Cengage Learning

Wu S, Zhu D, Li X, Li H, Lei J (2009) Thermal energy storage behavior of Al_2O_3–H_2O nanofluids. Thermochim Acta 483(1–2):73–77. https://doi.org/10.1016/j.tca.2008.11.006

Xu T, Zhao J, Xu K (1996) The ball-bearing effect of diamond nanoparticles as an oil additive. J Phys D Appl Phys 29:2932–2937. https://doi.org/10.1088/0022-3727/29/11/029

Yang L, Ji W, Mao M, Huang J-N (2020) An updated review on the properties, fabrication and application of hybrid-nanofluids along with their environmental effects. J Clean Prod. https://doi.org/10.1016/j.jclepro.2020.120408

Yıldız G, Ağbulut Ü, Gürel AE (2021) A review of stability, thermophysical properties and impact of using nanofluids on the performance of refrigeration systems. Int J Refrig 129:342–364. https://doi.org/10.1016/j.ijrefrig.2021.05.016

Yilmaz AC (2020) Performance evaluation of a refrigeration system using nanolubricant. Appl Nanosci 10(5):1667–1678. https://doi.org/10.1007/s13204-020-01258-5

Zawawi NNM, Azmi WH, Redhwan AAM, Sharif MZ, Sharma KV (2017) Thermo-physical properties of Al_2O_3-SiO_2/PAG composite nanolubricant for refrigeration system. Int J Refrig 80:1–10. https://doi.org/10.1016/j.ijrefrig.2017.04.024